

Matter rogue wave in Bose-Einstein condensates with attractive atomic interaction

Lin Wen¹, Lu Li², Zai-Dong Li³, Shu-Wei Song¹, Xiao-Fei Zhang¹, and W.M. Liu¹

¹*Beijing National Laboratory for Condensed Matter Physics,*

Institute of Physics, Chinese Academy of Sciences, Beijing 100080, China.

²*Institute of Theoretical Physics, Shanxi University, Taiyuan, 030006, China and*

³*Department of Applied Physics and School of Information Engineering,
Hebei University of Technology, Tianjin 300401, China*

We investigate the matter rogue wave in Bose-Einstein Condensates with attractive interatomic interaction analytically and numerically. Our results show that the formation of rogue wave is mainly due to the accumulation of energy and atoms toward to its central part; Rogue wave is unstable and the decay rate of the atomic number can be effectively controlled by modulating the trapping frequency of external potential. The numerical simulation demonstrate that even a small periodic perturbation with small modulation frequency can induce the generation of a near-ideal matter rogue wave. We also give an experimental protocol to observe this phenomenon in Bose-Einstein Condensates.

PACS numbers: 03.75.Kk, 03.75.Lm, 67.85.Hj

I. INTRODUCTION

The dynamics of Bose-Einstein condensates (BECs) at ultralow temperature are described well by Gross-Pitaevskii (GP) equation [1], in which the nonlinearity is arose from interatomic interactions characterized by the s-wave scattering length. Recently experiments have demonstrated that tuning of the effective scattering length, including a possibility to change its sign, can be achieved by using the so-called Feshbach resonance technique [2]. In particular, the experimental realization of BECs in dilute quantum gases have opened the floodgate in the field of atom optics and condensed matter physics [3]. At the same time, the collective excitation of matter waves in BECs has also drawn a great deal of interest to explore the dynamics of BECs deeply from both experimental and theoretical perspectives, such as matter wave solitons [4–9], periodic waves [10], shock waves [11], vortex [12] and necklaces [13]. However, to our knowledge less attention have been paid to the matter rogue wave which is a fundamental and novel nonlinear excitation in BECs.

Rogue waves from ocean are that their heights, from crest to trough, are more than about twice the significant wave height [14]. They appear without any warning and disappear without the slightest trace. Owing to severe environment and high risk in ocean, the systematic study of rogue waves become so difficult that the necessary conditions and physical mechanism of their generation are not sufficiently well understood. Recently, theoretical studies have shown that the rogue wave phenomenon can be explained well by nonlinear theories [15, 16], and the various possible formative mechanisms have been discussed, such as the modulation instability in one dimension [17, 18], nonlinear spectral instability [19] and in two-dimensional crossings [20]. Furthermore, the rogue waves phenomenon have been observed experimentally in variety of physical systems including optical fibers [21, 22], arrays of optical waveguide [23] and cap-

illary waves [24].

As a nonlinear physical system with similar nonlinear characteristics, BECs can support the interesting rogue waves and allow us to understand deeply the nature and the dynamics of rogue waves in laboratory conditions. The management of Feshbach resonance for nonlinearity and a tunable atomic trapping potential also provide us with a powerful tool for manipulating rogue wave. This enable BECs to have more advantages for investigating rogue wave than other physical media. In this paper, we mainly investigate the matter rogue wave of Peregrine type with the emphasis on its formative mechanism in BECs. We firstly obtain the exact rogue wave solution of the GP equation with time-dependent attractive atomic interaction in an expulsive parabolic potential. By analyzing the atomic number density distribution in the rogue wave against the background, the formative mechanism of matter rogue wave can be clarified that the accumulation of energy and atoms toward to its central part. Rogue wave can not keeps dynamic stability and the decay rate of the atomic number can be effectively controlled by modulating the trapping frequency of external potential. Moreover, we use the breather evolution in a regime approaching the excitation of matter rogue wave as approximation to simulate the creation of matter rogue wave numerically, which indicates that a small periodic perturbation with small modulation frequency can excite a near-ideal matter rogue wave. Finally, we also give a practical and effective experimental protocol to observe this interesting phenomenon in future BECs experiments.

II. MATTER ROGUE WAVE SOLUTION

Under the mean-field level, the evolution of macroscopic wave function of BECs obey the 3D GP equation [3]. For a cigar-shaped condensate at a relatively low density, when the energy of two body interactions is much

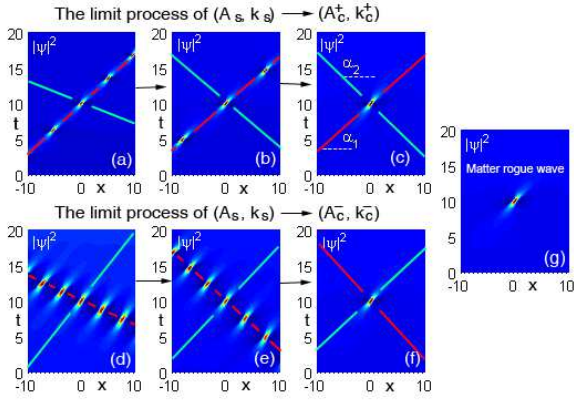


FIG. 1. (Color online) The asymptotic processes from Eq. (2) to Eq. (3) in the limitation of $(A_s, k_s) \rightarrow (2A_c, k_c)$. As the bright soliton amplitude A_s and wave number k_s approaching $(2A_c, k_c)$, the spatio-temporal separation between adjacent peaks gradually increases shown in Fig. 1(a-f), where the parameters are (a) $A_s = 2.4, k_s = 1.2$. (b) $A_s = 2.2, k_s = 1.2$. (c) $A_s = 2.01, k_s = 1.01$. (d) $A_s = 1.6, k_s = 0.8$. (e) $A_s = 1.8, k_s = 0.8$. (f) $A_s = 1.99, k_s = 0.99$. Fig. 1(g) represents the exact matter rogue wave solution Eq. (3) with $A_s = 2, k_s = 1$. Other parameters are $\lambda = 0.01, t_0 = 10, k_c = A_c = 1$. The red and green lines represent the sloping lines V_θ and V_α , respectively.

less than the kinetic energy in the transverse direction, the system can become effectively quasi-one-dimensional regime with time-dependent attractive interaction in an expulsive potential [25],

$$i \frac{\partial \psi}{\partial t} + \frac{1}{2} \frac{\partial^2 \psi}{\partial x^2} + a(t) |\psi|^2 \psi + \frac{1}{2} \lambda^2 x^2 \psi = 0, \quad (1)$$

where the aspect ratio reads $\lambda = |\omega_0|/\omega_\perp \ll 1$, coordinate x and time t are measured in units a_\perp and $1/\omega_\perp$ with $a_\perp = \sqrt{\hbar/m\omega_\perp}$ (m is the atomic mass) and $a_0 = \sqrt{\hbar/m\omega_0}$ the linear oscillator lengths in the transverse and cigar-axis directions, respectively. ω_\perp and ω_0 are corresponding harmonic oscillator frequencies. The nonlinear coefficient $a(t)$ is defined as $a(t) = |a_s(t)|/a_B$, where $a_s(t)$ is so-called s -wave scattering length. Corresponding to the real BECs experiment [9], the bright soliton can be created for ${}^7\text{Li}$ by tuning the scattering length continuously in an expulsive potential with $\omega_\perp = 2\pi \times 700\text{Hz}$ and $\omega_0 = 2i\pi \times 7\text{Hz}$. So we can choose the nonlinear coefficient in the form of $a(t) = \exp[\lambda(t-t_0)]$ manipulated by Feshbach resonance technique [26], where t_0 represents an arbitrary real constant determining the initial scattering length $|a_s(t=0)| = a_B e^{-\lambda t_0}$.

To obtain the exact solution of Eq. (1), we introduce the transformation $\psi = q(X, T) \exp[\lambda(t-t_0)/2 - i\lambda x^2/2]$ with the coordinate transformations $X = e^{\lambda(t-t_0)}x$ and $T = [e^{2\lambda(t-t_0)} - 1]/(2\lambda)$. Then Eq. (1) can reduce to the standard nonlinear Schrödinger equation, and the solution of Eq. (1) constructed on continuous wave (cw) background $\psi_{cw} = A_c e^{i\varphi}$ can be obtained as follows [27],

$$\psi = \left(A_c + A_s \frac{\chi \cosh \theta + \cos \alpha}{\cosh \theta + \chi \cos \alpha} + i A_s \frac{\eta \sinh \theta + \delta \sin \alpha}{\cosh \theta + \chi \cos \alpha} \right) \times \exp(i\varphi), \quad (2)$$

with

$$\chi = \frac{-2A_c A_s}{A_s^2 + M_R^2}, \quad \eta = \frac{-2A_c M_R}{A_s^2 + M_R^2}, \quad \delta = \frac{M_I}{A_s},$$

where $\theta = M_I X - [A_s M_R + (k_c + k_s) M_I] T/2$, $\alpha = M_R X - [(k_c + k_s) M_R - A_s M_I] T/2$, $\varphi = \varphi_c - \lambda x^2/2 - i\lambda(t-t_0)/2$, $\varphi_c = k_c X + (A_c^2 - k_c^2/2)T$ and $M_R + iM_I = \sqrt{(k_c - k_s - iA_s)^2 + 4A_c^2}$. The subscripts R and I denote the real and imaginary part of M , respectively.

In general, some excited state solutions, such as cw wave and bright soliton on the background of ground state, can be recovered successfully from Eq. (2). Firstly, when the cw background amplitude vanishes ($A_c = 0$), Eq. (2) reduces to the bright soliton solution $\psi_{sol} = A_s e^{i\varphi_s} \text{sech} \theta_s$ with varying amplitude $A_s e^{\lambda(t-t_0)}$ and group velocity $v_s = k_s \cosh[\lambda(t-t_0)]$ [28], where $\theta_s = A_s(X - k_s T)$ and $\varphi_s = k_s X + (A_s^2 - k_s^2)T/2$, and k_s represents the wave number of bright soliton. Secondly, when the initial amplitude of bright soliton vanishes ($A_s = 0$), Eq. (2) reduces to cw background solution $\psi_{cw} = A_c e^{i\varphi}$ with varying group velocity $v_c = k_c \cosh[\lambda(t-t_0)]$, where k_c is the wave number of cw background. So the exact solution Eq. (2) represents a bright soliton embedded in a cw background field. It should be pointed that the parameters A_c, A_s, k_c and k_s are derived from the mathematical construction of Eq. (2), the numerical values of these parameters can be chosen freely, so we assume that these parameters are real constants without loss of generality. Furthermore, the dynamical evolution of solution Eq. (2) are shown in Fig. 1(a-f). From Fig. 1 we observe that the solution in Eq. (2) commonly exhibits a breather characteristic and a time periodic modulation of the soliton amplitude, which can be regarded as the results of the interaction between the localized process of cw background along the slope direction V_α and the periodization process of bright soliton along the slope direction V_θ , i.e., the bright soliton undergo periodic energy and atoms exchange with cw background, where V_θ and V_α represent the lines $M_I X - [A_s M_R + (k_c + k_s) M_I] T/2 = 0$ and $M_R X - [(k_c + k_s) M_R - A_s M_I] T/2 = 0$ on the space-time plane as shown in Fig. 1, respectively.

Through above analysis we can see that when $k_c = k_s$, the bright soliton must move with the same group velocity as that of cw background which implies that the bright soliton and cw background are in ‘‘resonant state’’ in space. The critical point $A_s^2 = 4A_c^2$ forms the dividing line between modulation instability process ($A_c^2 > A_s^2/4$) and the periodization process of bright soliton ($A_c^2 < A_s^2/4$) under the resonant condition $k_c = k_s$ [27], which means that the relative initial intensity between the cw background and bright soliton determine the different

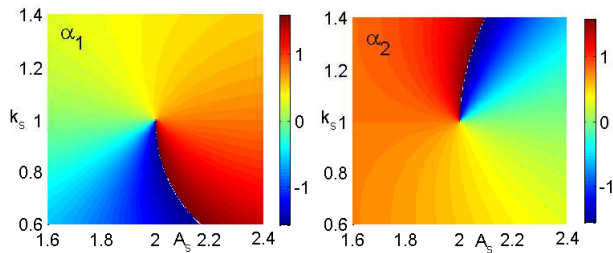


FIG. 2. (Color online) The plots for the evolutions of α_1 and α_2 as the function of A_s and k_s during the limit processes, where $k_c = 1$ and $A_c = 1$. The two angles α_1 and α_2 as the function of A_s and k_s are not continuous at the limit point.

physical behaviors of the solution Eq. (2). Especially, with the limit conditions of $k_c = k_s$ and $A_s^2 = 4A_c^2$, we have

$$\psi_R = \left[\frac{4 + i8A_c^2T}{1 + 4A_c^4T^2 + 4A_c^2(X - k_cT)^2} - 1 \right] A_c e^{i\varphi}, \quad (3)$$

which represents a localized matter wave with the maximal amplitude $A_P = 3A_c$ in BECs, and its dynamical evolution is shown in Fig. 1(g). Interestingly, the exact solution Eq. (3) displays the typical rogue wave characteristics of Peregrine type that a localized breather characteristic with only a single hump both in space and time, which indicates that the localized wave is captured completely at $x = 0$ and $t = t_0$ by the cw background [16]. So far, such solution Eq. (3) has been conjectured to be a prototype of oceanic rogue waves.

III. DYNAMICS OF MATTER ROGUE WAVE

In order to better clarify the formative mechanism of rogue wave solution in Eq. (3), we firstly investigate the asymptotic processes of Eq. (2) to Eq. (3) in the limit processes $(A_s, k_s) \rightarrow (2A_c, k_c)$ by fixing the numerical values of cw background amplitude A_c and wave number k_c . From Fig. 1(a-f), we can observe clearly that the spatio-temporal separation between adjacent peaks gradually increases as the bright soliton amplitude A_s and wave number k_s approaching $(2A_c, k_c)$, which leads to a greater spatio-temporal localization in Eq. (2). Furthermore, the parameters $\tan \alpha_1 = 2/(k_c + k_s + A_s M_R/M_I)$ and $\tan \alpha_2 = 2/(k_c + k_s - A_s M_I/M_R)$ shown in Fig. 1(c) represent the slope of the lines V_θ and V_α at $x = 0$ and $t = t_0$, respectively. When the values of A_s and k_s approaches to the critical point, V_θ and V_α gradually turn to a relative fixed direction associated with the maximal spatio-temporal localization in Eq. (2). However, the two angles α_1 and α_2 as the function of A_s and k_s are not continuous at the limit point shown in Fig. 2, i.e., α_1 and α_2 do not exist limitation, which play the important role to describe that the solution Eq. (2) is localized along V_θ and V_α at the limit point. Especially, rogue wave solution in Eq. (3) can be considered as a

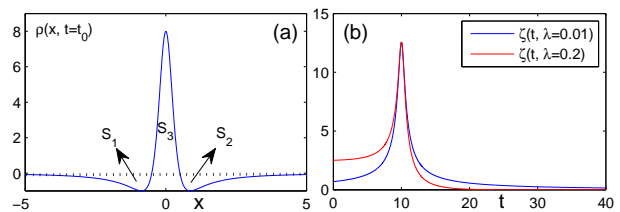


FIG. 3. (Color online) (a) The atomic number density distribution in matter rogue wave at fixed time point. (b) The atomic exchange between matter rogue wave and background. The parameters are $A_c = k_c = 1$ and $t_0 = 10$.

transition state between the modulation instability process ($A_s \rightarrow 2A_c^-$) and the periodization process of the bright soliton ($A_s \rightarrow 2A_c^+$) under the resonant condition $k_c = k_s$.

As shown in the following, the formation of rogue wave can be clarified by the atomic number density distribution against the background defined as $\rho(x, t) = |\psi_R(x, t)|^2 - |\psi_R(x = \pm\infty, t)|^2$. With Eq. (3), we have

$$\rho(x, t) = \frac{8A_c^2 + 32A_c^6T^2 - 32A_c^4(X - k_cT)^2}{[1 + 4A_c^4T^2 + 4A_c^2(X - k_cT)^2]^2} e^{\lambda(t-t_0)}, \quad (4)$$

and the time-independent integral $\int_{-\infty}^{+\infty} \rho(x, t) dx = 0$. From the condition $\rho(\pm 1/(2A_c), t_0) = 0$ and $\rho(0, t_0) = 8A_c^2$, one can define the spatial width of the hump part in rogue wave as $1/A_c$. At the fixed time $t = t_0$, we have integral $\int_{-1/(2A_c)}^{1/(2A_c)} \rho(x, t_0) dx = 4A_c$ and $\int_{-\infty}^{-1/(2A_c)} \rho(x, t_0) dx + \int_{1/(2A_c)}^{\infty} \rho(x, t_0) dx = -4A_c$. These results demonstrates clearly that for the attractive interatomic interaction, the generation of rogue wave with stronger breather characteristic is mainly due to the accumulation of energy and atoms toward to its central part. The time-independent area relation shown in Fig. 3(a), i.e., $S_1 + S_2 = S_3$, means that the loss of atoms in background completely transfer to the hump part of rogue wave. The forthcoming fundamental problem is that how rogue wave gather atoms and energy toward to its central part from the background. To this purpose, we investigate the exact number of atomic exchange between rogue wave and background which has the form

$$\zeta(t) = \int_{-\infty}^{\infty} |\psi_R(x, t) - \psi_R(\pm\infty, t)|^2 dx = \frac{4\pi A_c}{\sqrt{1 + 4A_c^4T^2}}. \quad (5)$$

From the above expression, we can see that $\zeta(t)$ is time-aperiodic which is different from periodic exchange of atoms between the bright soliton and the cw background in Eq. (2). As shown in Fig. 3(b), the atoms in background is gathered to the central part when $t < t_0$, which leads to the generation of a hump with two fillisters on the background along the space direction. The maximal peak of the hump and the deepest fillisters occur at $t = t_0$. However, the atoms in the hump start to spread

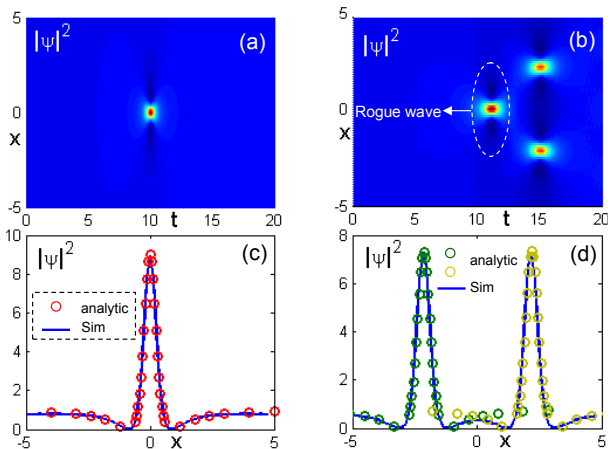


FIG. 4. (Color online) (a) Evolution of the exact rogue wave solution Eq. (3), where $A_c = 1$, $k_c = 0$, $\lambda = 0.01$ and $t_0 = 10$. (b) Evolution of the numerical solution of rogue wave with the initial condition Eq. (6), where $A_s = 1.92$, $\lambda = 0.01$, $t_0 = 10$. (c) and (d), The comparison of intensity profile between near-ideal rogue wave (in (c) with solid blue line) or sub-rogue wave pair (in (d) with solid blue line) and ideal rogue wave (circles).

into the fillisters when $t > t_0$. Therefore, the hump gradually decay which verifies that the rogue wave is only one oscillation in time and displays a unstable dynamical behavior.

Considering the dynamics of rogue wave in the background, on the one hand, a necessary condition for realizing rogue wave in experiment is that the scale of rogue wave must be very small compared with the length of the background of BECs. In the real experiments [8], the length of the background of BECs is at least $370\mu m$. At the same time, in Fig. 3(a), the actual width of rogue wave is about $10a_{\perp} = 14\mu m \ll 370\mu m$ (a unity of coordinate corresponds to $a_{\perp} = \sqrt{\hbar/m\omega_{\perp}} = 1.4\mu m$). Thus the rogue wave is observable experimentally. On the other hand, the decay rate of atoms in rogue wave can be controlled effectively by modulating the trapping frequency of external potential shown in Fig. 3(b). The decay time t_d is about $8.05ms$ for $\lambda = 0.01$ ($\omega_{\perp} = 2\pi \times 700Hz$ and $\omega_0 = 2i\pi \times 7Hz$ originate from the experiment [9]), while $t_d \approx 2.30ms$ for $\lambda = 0.2$ ($\omega_{\perp} = 2\pi \times 700Hz$ and $\omega_0 = 4i\pi \times 70Hz$), which demonstrate that a trap with small trapping frequency is conducive to the observation of matter rogue wave in BECs experiments.

A question arises about the possibility of the creation of such a matter rogue wave experimentally. Generally, the excitation of rogue wave can be recovered by means of the numerical simulation with some particular initial conditions [29]. From the experimental points of view, optimal initial conditions are not only conducive to the experimental preparation, but it is also useful for understanding the necessary conditions and physical mechanism of the generation of rogue wave. In what follows, we will look for the optimal initial conditions which can excite the resemble physical behavior of rogue wave.

By comparing the Fig. 1(c) and (f) with Fig. 1(g), Eq. (2) with infinity oscillation period is a very good approximation of rogue wave solution Eq. (3), this parameter regime yields characteristic rogue wave features in the spatio-temporal envelope even though the ideal rogue wave solution exists only asymptotically in the limitation of $A_c = 2A_s$ and $k_c = k_s$. Based on modulation instability mechanism in ultracold atom system [30], we consider the case of $A_c^2 > A_s^2/4$ with $k_s = k_c = 0$ corresponding to the modulation instability process of cw background. In this case, we can take $T \approx -t_0$ at $t = 0$ for a very small quantity λ , and the suitable values of A_s and A_c can ensure $\theta \approx t_0 A_s M_R/2$ to be so large that $\kappa = e^{-\theta}$ is a small quantity. By linearizing the initial value with the small quantity κ in Eq. (2) we get

$$\psi(x, 0) = (\sigma + \gamma\kappa \cos \alpha_0) e^{i\varphi(x, 0)}, \quad (6)$$

where $\sigma = (2A_c^2 - A_s^2 - iA_s M_R)/(2A_c)$, $\gamma = A_s M_R (M_R - iA_s)/(2A_c^2)$ and $\alpha_0 = M_R e^{-\lambda t_0} x$, $\varphi_c \approx -A_c^2 t_0$ and the modulation frequency of initial condition Eq. (6) is $\Omega = M_R e^{-\lambda t_0}$. The solution of initial value problem associated with Eq. (1) with initial condition Eq. (6) can be described well by the exact solution Eq. (2) [27]. For the creation of rogue wave, we require the value of $A_s/2$ to approach A_c associated with a very small modulation frequency in Eq. (6). The numerical results are shown in Fig. 4(b), which demonstrates that a small periodic perturbation with a very small modulation frequency can induce a near-ideal rogue wave localization, whose profile is basically consistent with the ideal theoretical limit solution Eq. (3) as shown in Fig. 4(a) and (c). However, the obvious difference is that owing to the actions of modulation instability and instability of rogue wave, the initial near-ideal rogue wave can break up into two lower amplitude but equally strongly localized sub-rogue wave, and each sub-rogue wave itself exhibits ideal rogue wave characteristics as shown in Fig. 4(d), which agrees well with the optical experimental conclusions [21, 22]. As a result, a small initial periodic perturbation with a small modulation frequency can induce the generation of a near-ideal rogue wave by the modulation instability mechanism in BECs.

Inspired by the experiments [7–9], we can design the following experimental steps to observe the interesting rogue wave phenomenon in BECs: (i) Creating a condensates of 7Li with total number of particles $N \approx \times 10^3$ and continuous wave phase distribution by using quantum phase imprinting technique and amplitude engineering; (ii) Loading the condensates into a slightly expulsive harmonic potential with the parameters $\omega_{\perp} = 2\pi \times 700Hz$ and $\omega_0 = 2i\pi \times 7Hz$, and ramping up the scattering length in the form of $a_s(t) = -0.9a_{BE}e^{\lambda t}$; (iii) Optimal initial state Eq. (6) can be produced by imprinting a periodic perturbation laser with very small modulating frequency onto condensates. The main effect of this expulsive term is that the center of the condensates accelerates along the longitudinal direction. In addition, a crucial question is that since we require the scattering

length to change over time in above experimental protocol, we must ensure the validity of quasi-one-dimensional regime and avoid the collapse of condensates with attractive interaction. In other words, we must ensure that the energy of two body interactions is much less than the kinetic energy in the transverse direction, i.e., $\varepsilon^2 \sim N|a_s|/a_0 \ll 1$. With initial scattering length $a_s(t=0) = -0.9a_B$, we can obtain $\varepsilon^2 \approx 0.03 \ll 1$. After about 50 dimensionless units of time, the scattering length becomes $|a_s(t)| = 1.4a_B$ corresponds to $\varepsilon^2 \approx 0.057 \ll 1$. So the validity of quasi-one-dimensional system can be maintained well. Finally, we emphasize that the interesting phenomenon of rogue wave can be observed within current experimental capability.

IV. CONCLUSIONS

In conclusion, we have investigated the formative mechanism of matter rogue wave in BECs with time-dependent interaction in an expulsive parabolic potential,

analytically and numerically. The generation of rogue wave with stronger breathing characteristic is mainly due to the accumulation of energy and atoms toward to its central part. Rogue wave can not keeps dynamic stability because of the aperiodic exchange of energy and atoms with the background; The decay rate of the number of atoms in rogue wave can be controlled effectively by modulating the trapping frequency of the external potential. Our numerical results show that a small periodic perturbation with a smaller modulating frequency can induce the generation of the near-ideal rogue wave. Finally, we emphasize that the interesting phenomenon of rogue wave in BECs can be observed experimentally. Our work may facilitate the deeper studies of hydrodynamic rogue wave.

The authors thank Prof. Z. Y. Yan and B. Xiong for helpful discussions. This work was supported by the NSFC under grants Nos. 10874235, 10934010, 61078079, 60978019, 10874038 and the NKBRSCF under grants Nos. 2009CB930701, 2010CB922904 and 2011CB921502, NSFC-RGC under grants Nos1386-N-HKU748/10, and the Hundred Innovation Talents Supporting Project of Hebei Province of China under Grant No. CPRC014.

-
- [1] L. Pitaevskii and S. Stringari, *Bose-Einstein Condensation* (Oxford University Press, New York, 2003).
- [2] J. L. Roberts *et al.*, Phys. Rev. Lett. **81**, 5109 (1998); J. Stenger *et al.*, Phys. Rev. Lett. **82**, 2422 (1999).
- [3] F. Dalfovo, S. Giorgini, L. P. Pitaevskii, and S. Stringari, Rev. Mod. Phys. **71**, 463 (1999).
- [4] A. D. Jackson *et al.*, Phys. Rev. A **58**, 2417 (1998); A. E. Muryshev *et al.*, Phys. Rev. A **60**, R2665 (1999); P. O. Fedichev *et al.*, Phys. Rev. A **60**, 3220 (1999); Th. Busch *et al.*, Phys. Rev. Lett. **87**, 010401 (2001).
- [5] W. P. Zhang *et al.*, Phys. Rev. Lett. **72**, 60 (1994); R. Dum *et al.*, Phys. Rev. Lett. **80**, 2972 (1998); X. F. Zhang *et al.*, Phys. Rev. A **77**, 023613 (2008).
- [6] Z. X. Liang *et al.*, Phys. Rev. Lett. **94**, 050402 (2005); B. Li *et al.*, Phys. Rev. A **78**, 023608 (2008); H. Saito *et al.*, Phys. Rev. Lett. **90**, 040403 (2003).
- [7] S. Burger *et al.*, Phys. Rev. Lett. **83**, 5198 (1999); J. Denschlag *et al.*, Science **287**, 97 (2000).
- [8] K. E. Strecker, G. B. Partridge, A. G. Truscott, and R. G. Hulet, Nature (London) **417**, 150 (2002).
- [9] L. Khaykovich, F. Schreck, G. Ferrari, T. Bourdel, J. Cubizolles, L. D. Carr, Y. Castin, and C. Salomon, Science **296**, 1290 (2002).
- [10] F. Kh. Abdullaev *et al.*, Phys. Rev. Lett. **90**, 230402 (2003).
- [11] V. M. Perez-Garcia, V. V. Konotop and V. A. Brazhnyi, Phys. Rev. Lett. **92**, 220403 (2004).
- [12] B. P. Anderson *et al.*, Phys. Rev. Lett. **86**, 2926 (2001).
- [13] G. Theocharis *et al.*, Phys. Rev. Lett. **90**, 120403 (2003).
- [14] C. Kharif and E. Pelinovsky, Eur. J. Mech. B/Fluids **22**, 603 (2003); P. Müller, Ch. Garrett, and A. Osborne, Oceanogr. **18**, 66 (2005).
- [15] A. R. Osborne, Mar. Struct. **14**, 275 (2001).
- [16] D. H. Peregrine, J. Austral. Math. Soc. **25**, 16 (1983).
- [17] K. L. Henderson, K. L. Peregrine, J. W. Dold, Wave Motion **29**, 341 (1999).
- [18] M. Onorato, A. R. Osborne, M. Serio, S. Bertone, Phys. Rev. Lett. **86**, 5831 (2001).
- [19] P. A. E. M. Janssen, J. Phys. Oceanogr. **33**, 863 (2003).
- [20] M. Onorato, A. R. Osborne, M. Serio, Phys. Rev. Lett. **96**, 014503 (2006); P. K. Shukla, I. Kourakis, B. Eliasson, M. Marklund, L. Stenflo, Phys. Rev. Lett. **97**, 094501 (2006).
- [21] D. R. Solli *et al.*, Nature **450**, 1054 (2007); D. -I. Yeom *et al.*, Nature (London) **450**, 953 (2007).
- [22] B. Kibler *et al.*, Nature Phys. **6**, 790 (2010); K. Hammani *et al.*, Opt. Lett. **36**, 112 (2011).
- [23] Yu. V. Bludov, V. V. Konotop, N. Akhmediev, Opt. Lett. **34**, 3015 (2009).
- [24] M. Shatz, H. Punzmann, H. Xia, Phys. Rev. Lett. **104**, 104503 (2010).
- [25] G. Fibich *et al.*, Phys. Rev. Lett. **90**, 203902 (2003); P. G. Kevrekidis *et al.*, Mod. Phys. Lett. B **18**, 173 (2004).
- [26] P. G. Kevrekidis *et al.*, Phys. Rev. Lett. **90**, 230401 (2003).
- [27] L. Li *et al.*, Opt. Commun. **234**, 169 (2004); Q. Y. Li *et al.*, Opt. Commun. **283**, 3361 (2010).
- [28] V. N. Serkin, A. Hasegawa, T. L. Belyaeva, Phys. Rev. Lett. **98**, 074102 (2007).
- [29] N. Akhmediev, J. M. Soto-Crespo, and A. Ankiewicz, Phys. Rev. A **80**, 043818 (2009).
- [30] L. D. Carr and J. Brand, Phys. Rev. Lett. **92**, 040401 (2004); L. Salasnich, A. Parola, and L. Reatto, Phys. Rev. Lett. **91**, 080405 (2003).